

Natures of a clump-origin bulge: a pseudobulge-like but old metal-rich bulge

Shigeki Inoue^{1,2*} & Takayuki R. Saitoh³

¹*Astronomical Institute, Tohoku University, Sendai 980-8578, Japan*

²*Mullard Space Science Laboratory, University College London, Holmbury St. Mary, Dorking, Surrey, RH5 6NT*

³*Interactive Research Center of Science, Tokyo Institute of Technology, 2-12-1 Ookayama, Meguro, Tokyo 152-8551, Japan*

2011 June 16

ABSTRACT

Bulges in spiral galaxies have been supposed to be classified into two types: classical bulges or pseudobulges. Classical bulges are thought to form by galactic merger with bursty star formation, whereas pseudobulges are suggested to form by secular evolution due to spiral arms and a barred structure funneling gas into the galactic centre. Noguchi (1998, 1999) suggested another bulge formation scenario, ‘clump-origin bulge’. He demonstrated using a numerical simulation that a galactic disc suffers dynamical instability to form clumpy structures in the early stage of disc formation since the premature disc is expected to be highly gas-rich, then the clumps are sucked into the galactic centre by dynamical friction and merge into a single bulge at the centre. This bulge formation scenario, which is expected to happen only at the high-redshift, is different from the galactic merger and the secular evolution. Therefore, clump-origin bulges may have their own unique properties. We perform a high-resolution N -body/smoothed particle hydrodynamics (SPH) simulation for the formation of the clump-origin bulge in an isolated galaxy model and study dynamical and chemical properties of the clump-origin bulge. We find that the clump-origin bulge resembles pseudobulges in dynamical properties, a nearly exponential surface density profile, a barred boxy shape and a significant rotation. We also find that this bulge consists of old and metal-rich stars, displaying resemblance to classical bulges. These natures, old metal-rich population but pseudobulge-like structures, mean that the clump-origin bulge can not be simply classified into classical bulges nor pseudobulges. From these results, we discuss similarities of the clump-origin bulge to the Milky Way bulge. Combined with a result of Elmegreen et al. (2008), this pseudobulge-like clump-origin bulge could be inferred to form in clump clusters with a relatively low surface density.

Key words: methods: numerical – galaxies: formation – galaxies: bulges – Galaxy: bulge – Galaxy: disc – Galaxy: formation.

1 INTRODUCTION

Kormendy & Kennicutt (2004) has suggested that bulges in spiral galaxies can be classified into *classical bulges* or *pseudobulges*. Classical bulges are thought to form through violent dynamical relaxation by galactic merger like elliptical galaxies (e.g. Nakasato & Nomoto 2003; Kormendy & Kennicutt 2004; Naab & Trujillo 2006; Rahimi et al. 2010; Hopkins et al. 2010). In other words, both of classical bulges and ellipticals could be merger remnants of galaxies, therefore supposed to be structurally identical. Indeed, their surface density profiles follow the $R^{1/4}$ law (de Vaucouleurs 1948), their shapes

are rounder than pseudobulges and they have little net rotation. Since the galactic merger is expected to consume most of gas in bursty star formation, the systems evolve passively and tend to be a single population system of old stars. The rapid star formation leads the enhancement of α -elements and makes the bulge metal-rich (Kormendy & Kennicutt 2004, and references therein). It is well known that classical bulges and ellipticals compose an identical fundamental plane and luminosity-metallicity relation (e.g. Kormendy & Illingworth 1983; Kormendy 1985; Jablonka et al. 1996; Burstein et al. 1997)

Pseudobulges are discussed to form through secular evolution caused by non-axisymmetric structures in a galactic disc, such as spiral arms and a barred structure (e.g. Combes & Sanders 1981; Pfenniger & Norman

* E-mail:inoue@astr.tohoku.ac.jp

1990; Combes & Elmegreen 1993; Bekki & Freeman 2002; Debattista et al. 2004; Athanassoula 2005). These non-axisymmetric structures rearrange angular momentum of the gas in a disc, funnel the gas into the galactic centre, which is presumed to arouse slow but long-lasting star formation resulting in a pseudobulge formation. Therefore, pseudobulges display a wide variety in their stellar population. As Kormendy & Kennicutt (2004) has speculated that pseudobulges retain a memory of their discy origin, observations indeed show disc-like natures of pseudobulges, such as an exponential surface density profile, a significant rotation, a flatter shape than those of classical bulges and frequent existence of nuclear structures (e.g. bar, spiral and ring).

However, some bulges can not be simply classified into the two types above. The bulge of the Milky Way (MW) would be a typical example. Some observations have proposed a nearly exponential surface density profile, an oblate peanut shape (X-shape) and a significant rotation in the MW bulge, indicating the pseudobulge signatures (e.g. Kent et al. 1991; Kent 1992; Dwek et al. 1995; Wyse et al. 1997; Kormendy & Kennicutt 2004, and references therein; Babusiaux et al. 2010; Nataf et al. 2010; McWilliam & Zoccali 2010; Saito et al. 2011; Nataf & Udalski 2011; Gonzalez et al. 2011b). The MW bulge also has characteristic properties of classical bulges. It has long been known that the MW bulge consists of old stars of which ages are suggested to be approximately 11 – 13 Gyr although uncertainty is still large (e.g. Terndrup 1988; Wyse et al. 1997; Kormendy & Kennicutt 2004, and references therein; Sahu et al. 2006; Bensby et al. 2010b, 2011b). Additionally, rapid star formation episode were also suggested by metal-rich nature and an overabundance of α -elements in the MW bulge (e.g. Wyse et al. 1997; Kormendy & Kennicutt 2004, and references therein; Ferreras et al. 2003; Nagashima & Okamoto 2006; Zoccali et al. 2006, 2008; Rich et al. 2007; Fulbright et al. 2007; Meléndez et al. 2008; Ryde et al. 2010; Bensby et al. 2010b, 2011b; Johnson et al. 2011; Hill et al. 2011). Thus, these observations seem to indicate that the MW bulge can not be simply classified into classical nor pseudobulges. In addition, recent observations argued that some bulges, which were classified into pseudobulges, display exceptionally inactive star formation like classical bulges (Drory & Fisher 2007; Fisher et al. 2009; Fisher & Drory 2010). These inactive pseudobulges are also unclassifiable bulges.

Noguchi (1998, 1999) has proposed another bulge formation scenario: ‘*clump-origin bulge*’. He demonstrated with numerical simulations that since galactic discs are expected to be highly gas-rich in early stage of the disc formation, clumpy structures form due to instability of the gas in the gaseous disc, which could also explain some clumpy galaxies observed in the high-redshift Universe (e.g. Noguchi 1998, 1999; Immeli et al. 2004a,b; Bournaud et al. 2007; Agertz et al. 2009; Aumer et al. 2010; Ceverino et al. 2010, 2011). These galaxies are referred to as clump clusters (chain galaxies) in the face-on (edge-on) view (e.g. van den Bergh et al. 1996; Elmegreen et al. 2004, 2009; Genzel et al. 2011). Noguchi (1998, 1999) suggested that these clumpy stellar structures fall into the galactic centre by dynamical friction and merge into a single bulge at the galactic centre, being clump-origin bulge.

Clump-origin bulges form through ‘*mergers of the clumps*’ in a galactic disc, neither the galactic mergers nor the secular evolution. Therefore, properties of clump-origin bulges could be different from those of the conventional ones. Since the simulations of Noguchi (1998, 1999) have been performed with a low resolution, he could not discuss the detailed properties of the clump-origin bulge (Noguchi, private communication). A few following studies discussed properties of the clump-origin bulge. Elmegreen et al. (2008) argued with numerical simulations that the clump-origin bulges should be classified into classical bulges, since the bulges in their simulations have a density profile near to the $R^{1/4}$ law, a thick shape, and a slow rotation in stellar component although the clumps are fast rotating before the bulge formation. They suggested that initial *spin* angular momentum of the clumps is lost to disc and halo when the clump-origin bulge forms. Recently Ceverino et al. (2011) studied dynamical state of gas in clumps migrating toward the galactic centre and demonstrated with both analytical approach and cosmological simulations that the gas component in most of clumps are highly rotation supported. Moreover, they discussed from their simulation results that more massive clumps are more highly rotation supported in the gas component and mentioned that clumps which have experienced a merger with other clumps tend to be highly rotationally supported ones (see their §4.2). These results of Ceverino et al. (2011) imply that the clump merger spins up the gas in the remnant clump. Since the clump-origin bulge is the final remnant of the clump mergers, we expect that the clump-origin bulges might be rotating fast like pseudobulges. However, they did not discuss the final structure of the bulge or dynamical state of the stellar component.

We perform a similar (but more sophisticated and much higher resolution) numerical simulation to Noguchi (1998, 1999) using an isolated galaxy model and study the naive natures of clump-origin bulges in details. We reconsider the rotation of the clump-origin bulge mentioned above, finally discuss similarity of the clump-origin bulge to the MW bulge. We describe our simulation settings in §2 and the results of the bulge properties in §3, including dynamical state, stellar age, metallicity and star formation activity. We present discussion in §4 and summary of our results in §5

2 SIMULATION

The detailed description of our computing schemes and initial conditions has been presented in Inoue & Saitoh (2011). We describe it briefly here.

We use an N -body/SPH code, ASURA (Saitoh et al. 2008, 2009). Gas dynamics is handled by the standard SPH scheme (Monaghan 1992; Springel 2010). We here adopt an individual time-step scheme, the time-step limiter of Saitoh & Makino (2009) to solve the evolution of the gas in the shocked regions correctly and the FAST method (Saitoh & Makino 2010) which accelerates the simulations of self-gravitating gas by integrating the gravitational and hydrodynamical parts with different time-steps. Gravity is solved by a parallel tree with GRAPE (GRAVity PipE) method (Makino 2004). We employ a barycentre approximation and the tolerance parameter of 0.5.

Cooling function of gas is assumed to be an optically

thin radiative cooling, depending on metallicity and covers a wide temperature range of $10 - 10^8$ K (Wada et al. 2009). Feedback from a uniform far-ultraviolet radiation and type-II supernovae (SNe) are also taken into account. A gas particle spawns a stellar particle of which mass is set to 1/3 of the mass of the original gas particle under the criteria: 1) $\rho_{\text{gas}} > 100 \text{ atm cm}^{-3}$, 2) temperature $T < 100$ K, 3) $\nabla \cdot \mathbf{v} < 0$ and 4) there is no SN around the particle. The local star formation rate is assumed to follow the Schmidt law (Schmidt 1959). The non-dimensional star formation efficiency is set to $C_* = 0.033$. Note that the global properties of star formation are fairly insensitive to the adopted value of C_* when one adopts a high mass resolution ($\sim 10^3 M_\odot$) and a high threshold density for star formation such as $\rho_{\text{gas}} > 100 \text{ atm cm}^{-3}$ (Saitoh et al. 2008). We assume the Salpeter initial mass function (Salpeter 1955) ranging from $0.1 M_\odot$ to $100 M_\odot$ on a stellar particle. We assume that stars heavier than $8 M_\odot$ cause type-II SNe and thermally heat up ambient gas (see also §3.3).

Our initial condition follows the spherical model of Kaufmann et al. (2006, 2007) that was used to study the formation of disc galaxies in an isolated environment. We assume an equilibrium system with the Navarro-Frenk-White profile (Navarro et al. 1997) with a virial mass $M_{\text{vir}} = 5.0 \times 10^{11} M_\odot$, a virial radius $r_{\text{vir}} = 1.67 \times 10^2$ kpc and a concentration parameter, $c = 6.0$. Baryon mass fraction of the system is set to 0.06. Initially all of baryon is primordial (zero-metal) gas having a virial temperature. The density profiles of dark matter (DM) and gas components are initially the same. The gas sphere has a rotation following a specific angular momentum distribution of $j \propto r$ (Bullock et al. 2001) normalized by a spin parameter of $\lambda = 0.1$. The DM halo is represented by 10^7 particles with a softening length of $\epsilon_{\text{DM}} = 8$ pc, whereas the gas in the halo is expressed by 5.0×10^6 particles with $\epsilon_{\text{gas}} = 2$ pc. The masses of DM and gas particles are $4.7 \times 10^4 M_\odot$ and $6.0 \times 10^3 M_\odot$, respectively.

Although we solve the wide temperature range of the inter-stellar matter (ISM), $T = 10 - 10^8$ K, we adopt neither temperature nor pressure floor. This is because we think these artificial suppression techniques of the low Jeans mass objects are unnecessary. It is widely believed that insufficient mass resolution may lead to unphysical fragmentation in the ISM. To avoid this ‘unphysical fragmentation’, one may adopt temperature/pressure floors which can maintain the condition of $M_{\text{Jeans}} > N_{\text{nb}} \times m_{\text{gas}}$, where M_{Jeans} is the Jeans mass, N_{nb} is the number of neighbouring SPH particles and m_{gas} is the mass of a gas particle. Since the original claim of the unphysical fragmentation was done based on their simulations during non-linear evolutions (Bate & Burkert 1997), it is hard to clarify what was the true origin of the unphysical fragments. This problem has been first pointed out by Bate & Burkert (1997). Since their evaluation was based on their simulation during non-linear evolutions, it is difficult to clarify what was the actual origin of the unphysical fragments.

Hubber et al. (2006) showed with well-conceived numerical tests for this problem that the growth of a linear-regime perturbation in a self-gravitating fluid is just slower than that of the analytical solution when the mass resolution is insufficient to express the local Jeans mass ($M_{\text{Jeans}} > N_{/r_{\text{mnb}}} \times m_{\text{gas}}$). They did not find any unphysical fragmenta-

tion in simulations with insufficient mass resolution. Therefore, there is no need to worry about the unphysical fragmentation in simulations with insufficient mass resolution without temperature/pressure floor. Hence, the result that the disk holds a number of small clumps especially in early phase in our simulation is not a numerical artifact (see, §3).

The effect of the insufficient mass resolution in our simulation would appear as the suppression of growth rates of clump seeds. However, this is not crucial for our results because (1) the dynamical time of seeds we may drop in our simulation is short because they are compact (2) the final mass of the clumps are much larger than the resolution limit.

3 RESULTS

We run the simulation for 6 Gyr and display snapshots of stellar and gas distributions and star forming region in Fig. 1. The simulated galaxy settles into a stable state after 5 Gyr.

At $t \lesssim 2$ Gyr, many clumps form in the disc onto which the surrounding gas is falling. Active star formation can be seen only in the clumps, whereas little star formation is found in the inter-clump (disc) region (the third row). This clumpy phase is seen in previous numerical studies and suggested to explain the clump clusters and chain galaxies observed in the high-redshift Universe (e.g. Noguchi 1998, 1999; Immeli et al. 2004a,b; Bournaud et al. 2007; Agertz et al. 2009; Ceverino et al. 2010, 2011; Aumer et al. 2010). In our simulation model, since the system is lacking continuous gas supply supposed in the cosmological context, the gas accretion ceases at $t \sim 2$ Gyr. After the cessation of gas supply, only a small number of tiny clumps form in the disc, which are fragile to tidal force and these disrupted clumps build up a stellar disc. The other massive clumps can survive, merge with one another and grow to more massive ones. In this phase, a central density slope of the DM halo is turned cored by the reaction of the dynamical friction on the clumps (Inoue & Saitoh 2011). The clumps are sucked into the galactic centre by dynamical friction and finally merge into a single ‘clump-origin’ bulge as first suggested by Noguchi (1998, 1999). At the final state ($t = 6$ Gyr), 80 per cent of the initial gas had converted into stars; the total stellar and gas masses are $2.5 \times 10^{10} M_\odot$ and $5.0 \times 10^9 M_\odot$, respectively. There is little gas in the halo region. The central density cusp of the DM halo is revived due to the gravitational potential of the massive bulge (Inoue & Saitoh 2011).

Noguchi (1996) has first suggested a thick disc formation scenario by dynamical heating on a disc by clumps, and Elmegreen & Elmegreen (2005) observationally discussed the existence of a thick disc in chain galaxies. Bournaud et al. (2009) demonstrated with numerical simulations that a disc forming in clump clusters is a thick disc, whereas a thin disc forms via gas accretion at the latter epoch than that of the thick disc formation. Since our simulation model does not take such a late stage accretion into account, we indeed find in our simulation that the disc is dominated by the thick disc component with a scale height of 1.41 kpc and a scale radius of 9.85 kpc, while a thin disc hardly forms. Therefore, in this paper, we consider the disc in our simulation to be a single-component thick disc which forms via the clumps. However, it does

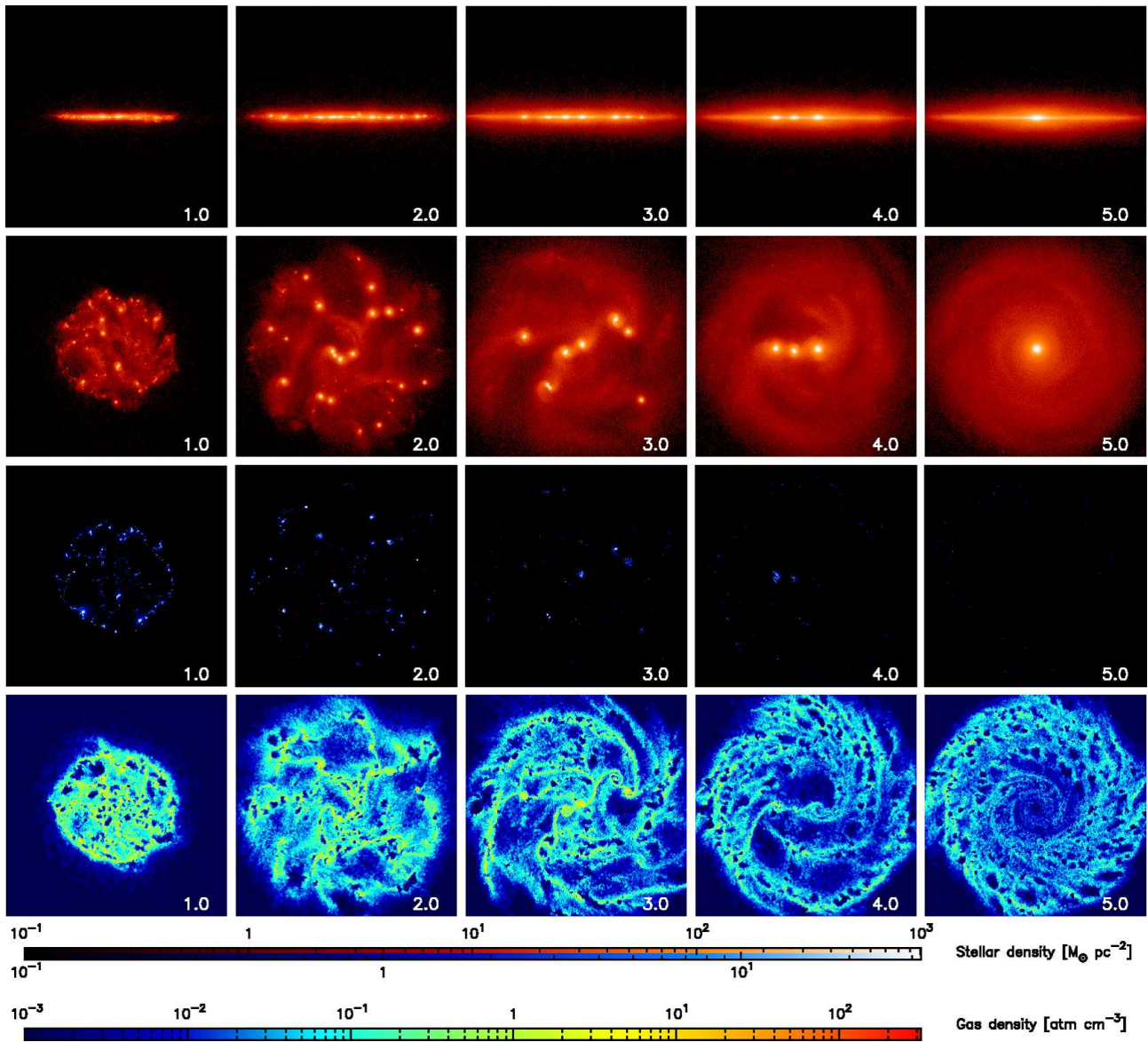


Figure 1. Stellar and gas density maps in the central 60×60 kpc region. The first and second rows indicate the surface density of all stars from the edge-on and face-on views, respectively. The third row plots the density of stars younger than 40 Myr as star forming region. The fourth row shows the volume density of gas in a slice of the disc plane. Time in unit of Gyr is indicated on right bottom in each panel.

not mean to reject other possible scenarios of thick disc formation, such as dissipative collapse (e.g. Burkert et al. 1992), thin disc heating (e.g. Quinn et al. 1993), accretion of dwarf galaxies (e.g. Abadi et al. 2003), multiple gas-rich minor merger (Brook et al. 2004, 2005) and radial migration (e.g. Sellwood & Binney 2002). We will report all the details of the thick disc formation and kinematics in our simulation in a forthcoming paper (Inoue & Saitoh, in prep).

In Fig. 2, we show the star formation history of the entire galaxy. Since the gas is continuously falling onto the galaxy ($t \lesssim 2$ Gyr), the system keeps star formation rate of $\sim 10 M_{\odot} \text{ yr}^{-1}$. After the gas infall phase, the galaxy asymptotically settles to the low star formation state with $\sim 1 - 0.1 M_{\odot} \text{ yr}^{-1}$. When the stellar clumps coalesce with one another, the star formation activity is temporarily activated

in the clusters, resulting in appearance of spiky features in the late history of star formation in Fig. 2.

3.1 Dynamical state

3.1.1 Density profile

In order to identify the bulge type, i.e. classical or pseudobulges, the Sérsic profile fitting of a surface density profile of bulge stars is frequently used:

$$\Sigma(R) = \Sigma_0 \exp \left[- \left(\frac{R}{R_0} \right)^{\frac{1}{n}} \right], \quad (1)$$

where Σ_0 and R_0 are the central surface density and the scale radius of the bulge, respectively, and n is the Sérsic index. If $n = 1$, the profile is consistent with an exponen-

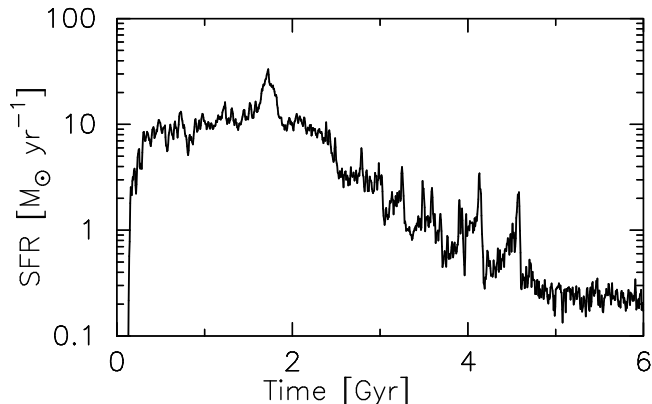


Figure 2. Star formation rate (SFR) as a function of time. The entire region of the galaxy is considered.

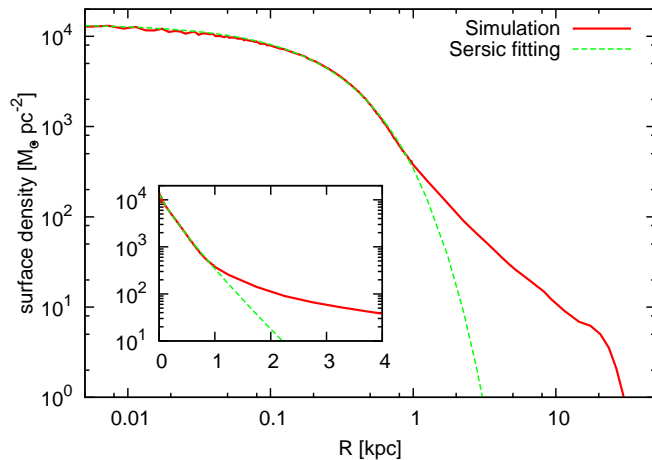


Figure 3. Stellar surface density profile from the face-on view at the final state of the simulation ($t = 6$ Gyr). Minimum χ^2 fitting by the Sérsic profile with the index, $n = 1.18$, is also plotted. The centre of the system is defined to be the densest point in the stellar density distribution. The insert diagram illustrates the same density profiles with the linear abscissa.

tial profile implying a pseudobulge. If $n = 4$, the profile follows the de Vaucouleurs’ $R^{1/4}$ law (de Vaucouleurs 1948) implying a classical bulge. The boundary is empirically set to $n \simeq 2$ with little overlap (e.g. Kormendy & Kennicutt 2004; Drory & Fisher 2007; Fisher & Drory 2008).

In Fig. 3, we plot the azimuthally averaged surface density of stars at the final state and the result of the Sérsic profile fitting. The fitting by minimum χ^2 is given by $\Sigma_0 = 1.37 \times 10^4 \text{ M}_\odot/\text{pc}^2$, $R_0 = 0.21$ kpc, and the Sérsic index, $n = 1.18$. This value of the index, n , means the bulge in our simulation has a nearly exponential surface density profile and indicates a pseudobulge-like density structure. Contrary to this, Elmegreen et al. (2008) has indicated with numerical simulations that their clump-origin bulges have a Sérsic index larger than 2 and the morphology of classical bulges. We will discuss this contradiction in §4.4.

The Sérsic profile can not fit the simulated profile outside $R \gtrsim 1$ kpc. We find the transition radius between the disc and the bulge components at $R \sim 1$ kpc on the surface density. Thus, we define the bulge region to be inside

$R = 1.0$ kpc. The bulge has a mass of $4.5 \times 10^9 \text{ M}_\odot$ and a half-mass radius of 450 pc. Ratio of the bulge mass to the total stellar mass, B/T , is 0.18^1 . However, it must be kept in mind that the galaxy in our simulation does not have a thin disc. Since a thin disc accounts for not a small fraction of stellar mass of a real galaxy, the B/T must be overestimated in our simulation. Fisher & Drory (2008) has observed the mean value of B/T to be $\langle B/T \rangle = 0.16 \pm 0.05$ among pseudobulges and $\langle B/T \rangle = 0.41 \pm 0.11$ among classical bulges. Therefore, the clump-origin bulge in our simulation is near to pseudobulges on the value of B/T .

It should be noted that the B/T could be sensitive to simulation setup. We speculate that the B/T would become smaller if the gas accretion onto the disc is slower, because wavelength at which instability first appears becomes smaller in a gas-poorer disc (Toomre 1964; Binny & Tremaine 2008), which allows to form smaller clumps preferentially. They tend to be disrupted by the galactic tide and/or lead to result in a smaller clump-origin bulge. On the other hand, if we assume a smaller spin parameter in the initial condition, the gas forms a smaller disc and the gas is more condensed in the disc than that in the current simulation (Fall & Efstathiou 1980; Baron & White 1987). In such cases, the wavelength of the instability becomes larger, the larger clumps would form and result in the formation of a larger bulge. In the dense and small disc, since the timescale of the clump migration becomes much shorter, the bulge formation would be finished earlier than the current simulation.

3.1.2 Shape

In Fig. 4, we show stellar surface density maps of the bulge at the final state in our simulation. As seen in the image from the face-on view (the top panel), the bulge has a bar-like elongated feature. This ‘nuclear bar’ in a bulge is a common feature among pseudobulges (e.g. Kormendy & Kennicutt 2004). Ellipticity² of the bulge measures 0.55 from the face-on view.

As seen from the edge-on view (the bottom panel), it clearly appears that this bulge is a boxy bulge, indicating a pseudobulge signature (e.g. Kormendy & Kennicutt 2004; Athanassoula 2005). Ellipticity of the bulge measures 0.67 from the edge-on view.

3.1.3 Rotation

Pseudobulges are generally observed to have a significant rotation (e.g. Kormendy & Kennicutt 2004, and references therein; Williams et al. 2011). On the other hand, classical bulges are generally presumed not to rotate significantly although some classical bulges show a net rotation (Kormendy & Illingworth 1982; Cappellari et al. 2007).

In Fig. 5, we illustrate a map of the mean line-of-sight (LoS) velocity of stars from the edge-on view (perpendicular

¹ For example, the MW has a value of $B/T = 0.19 \pm 0.02$ (Kent et al. 1991; Dwek et al. 1995).

² In this paper, the ellipticity is defined to be $1 - b/a$ of the isodensity contour at which the surface density is equal to $\Sigma_0/2$, where a and b are lengths of major- and minor-axes.

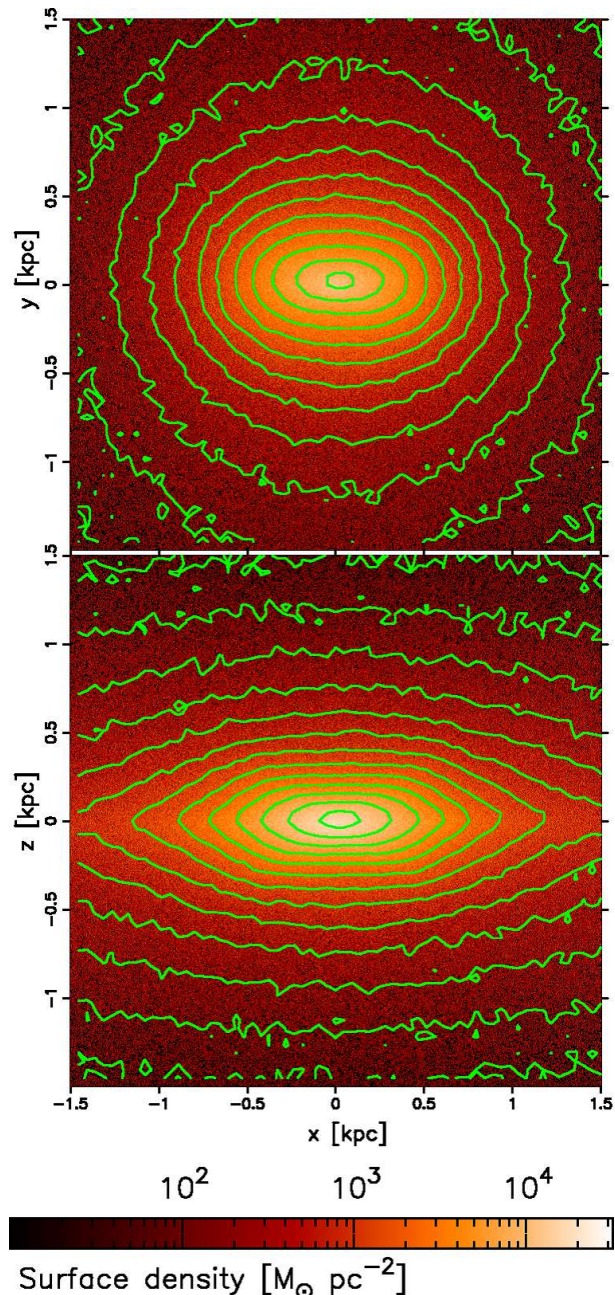


Figure 4. Stellar surface density maps in central 3×3 kpc region at the end-state of the simulation ($t = 6$ Gyr). The top panel is from the face-on view and the bottom one is from the edge-on view. The horizontal axes (x -axes) coincide with the major-axis of the bulge in both panels. The contour levels in the images are chosen to highlight the bulge shape.

to the major-axis) at the final state. The value is normalized by the LoS velocity dispersion interior to the half mass radius of the bulge (450 pc), $\sigma_0 = 81.0 \text{ km s}^{-1}$. This bulge shows a significant rotation. The value of $V_{\text{max}}/\sigma_0 \simeq 0.9$ of this bulge means that the rotation (spin) is *not* negligible but comparable to the velocity dispersion, where V_{max} is the maximum mean LoS velocity in the bulge. This is also a pseudobulge-like signature (Kormendy & Kennicutt 2004, and references therein). The direction of the rotation coincides with the disc rotation.

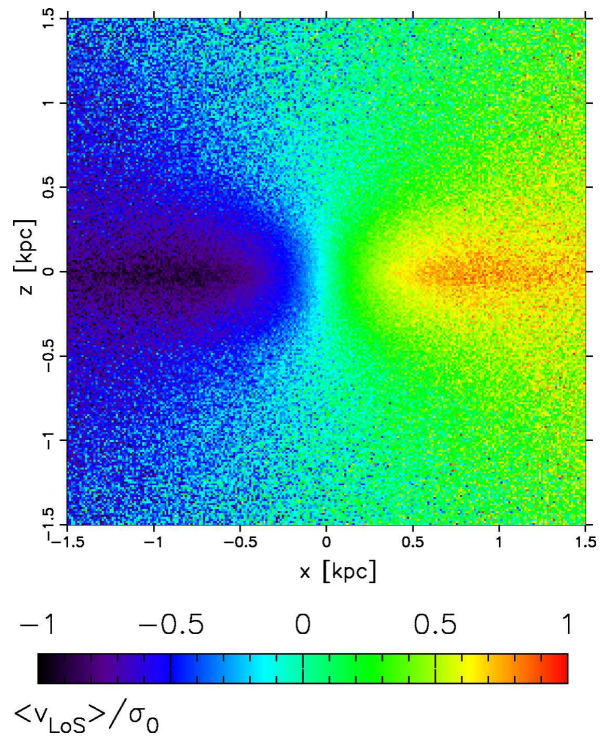


Figure 5. Mean LoS velocity map of the stellar component in the central 3×3 kpc region at the final state of the simulation ($t = 6$ Gyr) from the angle edge-on and perpendicular to the major-axis of the bulge. The value is normalized by the LoS velocity dispersion interior to the half mass radius of the bulge, $\sigma_0 = 81.0 \text{ km s}^{-1}$.

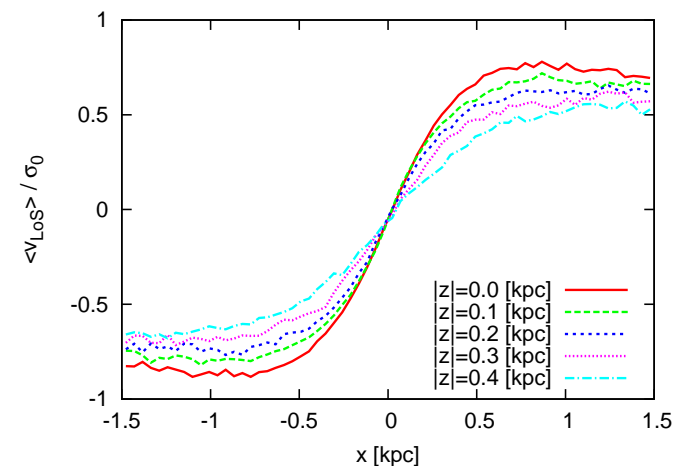


Figure 6. Rotation velocity curves at different heights above the disc plane, z . The abscissa coincides with the major axis of the bulge.

Recently, observations of some pseudobulges have shown that rotational velocities do not depend on a height within the bulges (Williams et al. 2011, and references therein), including the MW bulge (Howard et al. 2009), i.e. ‘*cylindrical rotation*’. However, regardless of our results that the clump-origin bulge follows the pseudobulge-like natures and the boxy morphology, we do *not* find a cylindrical rotation in the clump-origin bulge simulated in this work. Fig. 6

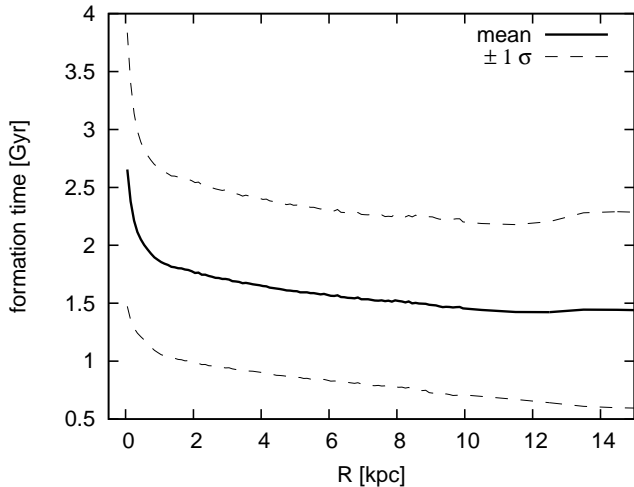


Figure 7. Averaged formation time of star particles as a function of the galactocentric distance. The values are azimuthally averaged and a dispersion, σ , is calculated in each radial bin. This is a formation time of stars, not age. We define the start of the simulation to be the zero-point of the formation time.

shows that the rotation velocity curves tend to be flatter at a higher latitude of the bulge. However, Williams et al. (2011) has observationally shown that boxy/peanut-shaped bulges do not necessarily involve a cylindrical rotation. Therefore, their result implies that the cylindrical rotation may not be a congenial nature of the boxy/peanut-shaped bulges.

Recently, Saha et al. (2011) indicated with a numerical simulation that interaction with a barred structure in a disc can spin up a non-rotating bulge and the bulge acquires a boxy/peanut shape and a cylindrical rotation. If this mechanism is efficient, the cylindrical rotation can be built up after the bulge established and may not be a strong indicator for the bulge formation mechanism.

3.2 Age

As we noted in §1, classical bulges are generally an old structure because the classical bulges form by past galaxy merger events. Therefore, their stellar evolution tends to be passive after the last merger. As for pseudobulges, their star formation is generally still going on (although see also §3.4) because non-axisymmetric structures continue to funnel gas into the central bulge. Hence, stellar age in a bulge is also another important indicator to identify the bulge type.

In Fig. 7, we plot the mean and dispersion of the formation time of stars in our simulation. As seen in the figure, the bulge ($R \lesssim 1$ kpc) is younger than the thick disc only by ~ 1 Gyr. It is because the clumps in the clump cluster retain star formation activity inside them (the third row of Fig. 1) and migrate to the galactic centre while forming new stars. The formation time of disc stars are almost independent from the distance from the galactic centre.

However, the difference in the formation time between the bulge and the disc, ~ 1 Gyr, is so small in comparison with the age of the Universe that we could presume the bulge to form simultaneously with the disc. As mentioned above, the disc in our simulation is a thick disc, does not have a thin disc. Moreover, this bulge formation scenario

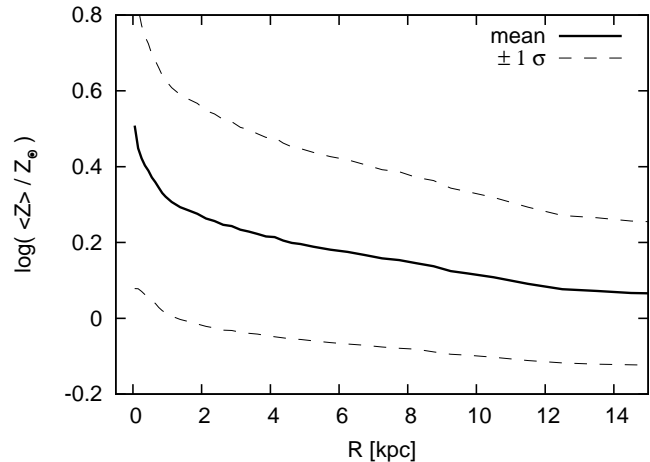


Figure 8. Radial metallicity distribution at $t = 6$ Gyr. The dashed lines indicate the range of $\pm 1\sigma$ dispersion. The value of solar metallicity, Z_{\odot} , is set to 0.02.

is expected to happen only in the high-redshift Universe. Therefore, we could consider that this clump-origin bulge is an old structure, as old as the thick disc.

To be an old structure *does* conflict with the morphological and dynamical similarities of this clump-origin bulge to pseudobulges mentioned in §3.1. Therefore, we suggest that the clump-origin bulge dynamically resembles pseudobulges but consists of the old stars like classical bulges. Hence, the clump-origin bulge can *not* be simply classified into classical bulges nor pseudobulges, but shows peculiar properties. However, we have to note that the bulge may be rejuvenated by the late accretion to form a thin disc.

3.3 Metallicity

Before discussing metallicity, we should describe here how we treat chemical evolution in our simulation. Our simulation code tracks only the total metal abundance, Z , and does not follow the evolution of each element. The initially primordial gas is contaminated with heavy elements by type-II SNe. We did not take type-Ia (or other) SNe or stellar wind from intermediate mass stars into account in our simulation.

We show a radial metallicity distribution in our simulation in Fig. 8. Stars of the clump-origin bulge are more metal-rich by 0.2 dex than stars of the inner region of the thick disc. Such a high metal abundance in the bulge is a natural outcome of the formation of clumps which form from a collapsing gas cloud in the highly gas-rich disc and the violent star formation in the clump mergers.

Recent observations have shown that there is no or little chemical distinction between the MW bulge and the thick disc stars in $[\alpha/\text{Fe}]$ vs. $[\text{Fe}/\text{H}]$ distributions despite exhibiting clear differences in their metallicity distribution functions (Meléndez et al. 2008; Bensby et al. 2009, 2010a,b, 2011b; Alves-Brito et al. 2010; Gonzalez et al. 2011a; Hill et al. 2011). However, observation results of Lecureur et al. (2007) and Fulbright et al. (2007) indicated clear separations of $[\alpha/\text{Fe}]$ between the thick disc and bulge stars in the MW. Observations of the chemical distinction between the MW bulge and the thick disc stars are still

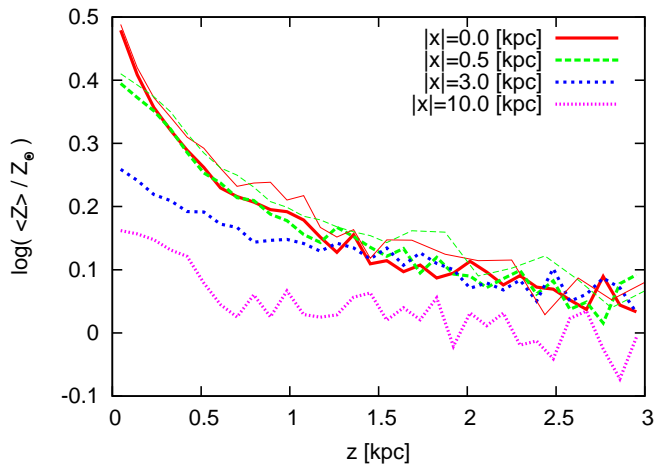


Figure 9. Vertical metallicity distribution at the bulge regions ($|x|=0.0$ kpc and 0.5 kpc) and disc regions ($|x|=3.0$ kpc and 10.0 kpc). Values are averaged along LoS. Thin lines (red solid and green long-dashed) indicate the metallicity distribution of the bulge stars only ($R < 1$ kpc).

controversial because of only a handful number of reliable sample stars and lack of accuracy of distances and proper motions to distinguish the bulge and disc stars³. Our simulation predicts the higher metallicity in the bulge than the thick disc. More convincing observations are highly anticipated to test such a scenario. Note, however, that there are many ways to build up thick discs, as we noted in §2.

Ruchti et al. (2011) recently observed that the MW thick disc shows a small radial gradients in $[\text{Fe}/\text{H}]$ ratio, $+0.01 \pm 0.04$ dex kpc^{-1} . Allende Prieto et al. (2006), Ivezić et al. (2008) and Bensby et al. (2011a) also observationally confirmed no or little radial $[\text{Fe}/\text{H}]$ gradient in the thick disc stars. Our result in Fig. 8 shows a small negative gradient, -0.014 dex kpc^{-1} , in metallicity, Z , from $R = 2.0$ kpc to 15.0 kpc, which is not inconsistent with these observations in the MW within the error.

It has been indicated that there is a clear variation in metallicity along the minor axis of the MW bulge (van den Bergh & Herbst 1974; Terndrup 1988; Frogel et al. 1990; Terndrup et al. 1990; Zoccali et al. 2008; Johnson et al. 2011; Gonzalez et al. 2011b). Zoccali et al. (2008) observed the vertical gradient of the mean $[\text{Fe}/\text{H}]$ ratio to be -0.6 dex kpc^{-1} . We here show metallicity distributions along the vertical direction in our simulation in Fig. 9. This figure clearly indicates a vertical metallicity gradient along the minor axis in the clump-origin bulge, $z \lesssim 1.0$ kpc of the solid red line. Contamination by the disc stars is negligible in the bulge region (the thin lines). In our result, the metallicity keeps increasing even in the central region of the clump-origin bulge although Rich et al. (2007) has observed no evidence for the vertical gradients of $[\text{Fe}/\text{H}]$ and $[\alpha/\text{Fe}]$ in the central region of the MW bulge, between $(l, b) = (1^\circ, -4^\circ)$ and $(l, b) = (0^\circ, -1^\circ)$ in the Galactic coordinate.

In the MW thick disc, Ruchti et al. (2011) observed

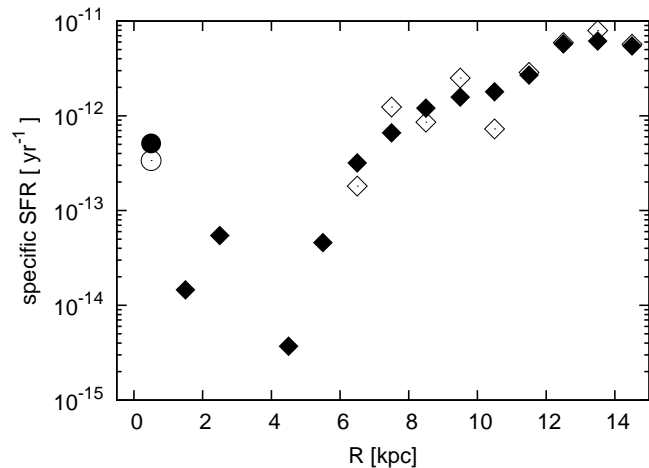


Figure 10. Specific star formation rate at the final state of the simulation ($t = 6$ Gyr). Filled and open symbols indicate values averaged in the last 0.5 Gyr and 40 Myr, respectively. Circles and diamonds indicate the values of the bulge and disc region, respectively. The open symbols are missing data points at inner disc region, $1 \text{ kpc} < R < 6 \text{ kpc}$, since no star particle was born in this radial range in the last 40 Myr.

that the vertical gradient of $[\text{Fe}/\text{H}]$ ratio is very small, -0.09 ± 0.05 dex kpc^{-1} . In our simulation, the vertical gradient of Z is small, ~ -0.05 dex kpc^{-1} in the thick disc region. Additionally, we find that the vertical metallicity gradients are almost independent of the galactocentric distance. This is represented in Fig. 9. The blue dotted line (inner disc region) and the purple dot-dashed line (outer disc region) are almost parallel.

3.4 Star formation activity

Classical bulges are supposed to have used up their gas and/or have a central massive black hole to heat up and prevent gas from accreting (Okamoto et al. 2008). Therefore, they are generally inactive in star formation. Pseudobulges are still forming stars actively, which is observationally verified by star forming nuclear rings nuclear spirals, bars and ovals, implying similarities to disc galaxies (e.g. Kormendy & Kennicutt 2004, and references therein; Fisher 2006; Fisher & Drory 2010).

In Fig. 10, we show the specific star formation rate⁴ in the bulge and the thick disc of our simulation. The clump-origin bulge is little forming stars at the final state. This bulge has very quiet and weak star formation activity. In the thick disc, the specific star formation rate becomes larger as R increases. The innermost region of the disc is less active than the bulge region. There is little difference between the values averaged in the last 40 Myr (the open symbols) and 0.5 Gyr (filled symbols). Thus, the inactive star formation is not transient. This halted star formation in the bulge is a typical feature of classical bulges.

Some bulges classified into pseudobulges are discovered to show inactive star formation like classical bulges

³ Hill et al. (2011) argued that using different reference stars in calibration was the cause of the conflict.

⁴ The specific star formation rate is defined in this paper as a star formation rate in a radial bin divided by the mass of the bin.

(Drory & Fisher 2007; Fisher et al. 2009; Fisher & Drory 2010). These bulges have a small value of the Sérsic index, $n \lesssim 2$, despite the fact that their star formation activity is as weak as classical bulges. These are called ‘inactive pseudobulges’ (Fisher et al. 2009; Fisher & Drory 2010). Although the bulge in our simulation is less active than the observed inactive pseudobulges by ~ 1 dex in the specific star formation rate ($\sim 10^{-11} \text{ yr}^{-1}$ in the observations), the clump-origin bulge in our simulation resembles to the inactive pseudobulges: the nearly exponential surface density and the inactive star formation.

We have to note that it could not be fair to directly compare the bulge in our simulation with the inactive pseudobulges in observations. The inactivity of these observed pseudobulges may be due to feedback from an active galactic nucleus, while our simulation does not take it into account. Moreover, the simulated galaxy is lacking the later gas accretion which would play an important role for the thin disc formation. The star formation activity in the clump-origin bulge would be affected by the gas accretion: a dynamically cold thin disc forms non-axisymmetric structures such as spiral arms and a galactic bar, which can supply the bulge with gas more or less and would activate the star formation in the bulge.

4 DISCUSSION

4.1 Validity of the model settings and comparison with observations

We set the larger spin parameter than the mean value of cosmological simulations, $\lambda \simeq 0.035$, (e.g. Bullock et al. 2001; Kimm et al. 2011) although observed values among high-redshift galaxies are still controversial (e.g. Bouché et al. 2007; Dutton et al. 2011). As we mentioned in §3.1.1, the large spin parameter would lead the formation of a large disc, small clumps and a small bulge. Elmegreen & Elmegreen (2005) observed that diameters of galactic discs range 13 – 29 kpc among 10 clump cluster samples of which masses are $0.5 - 25 \times 10^{10} M_{\odot}$. The numbers of clumps in the sample are 5 – 14 per galaxy and the averaged clump masses in the clump cluster range $0.21 - 1.36 \times 10^9 M_{\odot}$. The disc in our simulation is larger than their observational result by a factor of 2 or 3 and the surface density of inter-clump region is lower than the observed values (see also Elmegreen et al. 2009). Therefore, our simulation may *not* be a well-reproduced model of the high-redshift galaxies in the current observations on the points of the disc size and the surface density, although our simulation does not seem inconsistent with the observation of Elmegreen & Elmegreen (2005) on the points of the number and mass of the clumps (compare with 2 – 3 Gyr in Fig.1). In our simulation, the mass resolution of gas, which corresponds to the minimum resolved Jeans mass, is approximately $N_{\text{nb}} \times m_{\text{gas}} \simeq 2 \times 10^5 M_{\odot}$. This is much smaller than the mean clump masses observed in Elmegreen & Elmegreen (2005) and comparable to the smallest clumps in Elmegreen et al. (2009). Therefore, the mass and number of clumps we obtained in our simulation are do not suffer from the resolution effects.

However, current high-redshift observations still have difficulties of limited angular resolution and detectability,

which would have caused underestimates of the number of clumps and the disc diameter. Moreover, low luminosity clump clusters might have been missed. As discussed in Elmegreen et al. (2009), the current high-redshift observations would be biased to bright parts in bright galaxies. Elmegreen & Elmegreen (2005) discussed that their clump cluster samples have a too high inter-clump surface density to be a typical nearby spiral galaxy like the MW. Although clump clusters with a low surface brightness would not be the most representative cases for the high-redshift clump clusters, it may be possible that the low surface brightness clump clusters had been present but missed in the observations, and may be a progenitor of the nearby spiral galaxies. Our simulation result may corresponds to such a low luminosity clump cluster, which suggests the old and metal-rich pseudobulge formation from the clumps.

The longevity of the clumps in our simulation should be also examined carefully. In our simulation, the clumps take ~ 5 Gyr to merge into the bulge. The clump migrations in the previous simulations have accomplished in a shorter time, ~ 1 Gyr (e.g. Immeli et al. 2004a; Bournaud et al. 2007, 2009; Elmegreen et al. 2008; Aumer et al. 2010; Ceverino et al. 2011). The main causes of this difference are the disc size and the clump mass. The clumps in our simulation have to migrate a long distance to the galactic centre because of the larger disc scale length than that in the previous works. In addition, the clump masses seem somewhat smaller than these in the previous works. Therefore, the dynamical friction on the clumps is weak in our simulation.

In such a case of the slow evolution with the long-lived clumps, the clump clusters can not finish the formation of disc and bulge in the early Universe. If the evolution time scale is ~ 5 Gyr like our simulation, the clumps remain in galaxies until after the redshift $z \sim 1$. Observationally, there exists clump clusters even after the redshift $z \sim 1$, and Elmegreen et al. (2009) observed that the clump clusters in the lower-redshift Universe are less massive than these in the higher-redshift Universe although they discussed that this ‘downsizing’ is due to a detection limit in the observation and a smaller sampling volume in the lower-redshift Universe. If this downsizing is real, our simulation may correspond to such less massive galaxies evolving slowly until the low-redshift.

Disruption of the clumps should be also discussed. Recently, Genzel et al. (2011) has observed strong outflows from some clumps, which are faster than the escape velocity of the clump. Genel et al. (2010) demonstrated the clump disruption due to the superwinds implemented in their numerical simulations by a parametrised wind model, although Krumholz & Dekel (2010) had analytically discussed that such a strong feedback would not be realistic. The SN feedback model adopted in our simulation can not reproduce such destructive superwinds. Krumholz & Dekel (2010) suggested that the most probable engine of the superwinds is radiation pressure from newly formed massive stars. However, most of simulations for galaxy formation have not been implemented with the radiation pressure from the massive stars and our simulation did not either. The result of Genel et al. (2010) implies that taking the radiative feedback into account may drastically change the picture of the simulations for clump clusters.

4.2 Similarity to the MW bulge

The MW bulge does not follow the properties of classical bulges nor pseudobulges. The MW bulge shows a nearly exponential profile, an oblate peanut shape (X-shape) and a significant rotation, which are similar to pseudobulges. At the same time, it has old stars, a high metallicity and weak star formation, which are similar to classical bulges (e.g. Wyse et al. 1997; Kormendy & Kennicutt 2004, and references therein). These properties of the MW bulge are consistent with the clump-origin bulge obtained by our simulation although the absence of cylindrical rotation is inconsistent with the MW bulge.

Bulge stars of the MW are observed to be α -element enhanced (e.g. McWilliam & Rich 1994; Kormendy & Kennicutt 2004, and references therein; Zoccali et al. 2006, 2008; Lecureur et al. 2007; Fulbright et al. 2007; Meléndez et al. 2008; Alves-Brito et al. 2010; Hill et al. 2011). Interestingly, Zoccali et al. (2006) observationally discussed that an [O/Fe] vs. [Fe/H] distribution of the MW bulge stars agrees very well with the result of the chemo-dynamical simulation for clump-origin bulge formation in Immeli et al. (2004a). On the other hand, contrary to Zoccali et al. (2006), the recent observation of Baade’s window by Hill et al. (2011) showed considerable disagreement in a metallicity distribution function with the simulation result of Immeli et al. (2004a). These chemical abundances will provide further constraints on the bulge formation scenario.

We assumed an idealized simulation model, a collapsing gas sphere in a Navarro-Frenk-White model halo, in order to study *naive natures* of a clump-origin bulge. As we noted repeatedly in previous sections, our model would need the later gas accretion to form a thin disc (Bournaud et al. 2009). Moreover, in the cosmological context, real galaxies suffer galaxy merger more or less. These physical processes following the clump-origin bulge formation could alter the naive natures of the clump-origin bulge. For example, as we noted in §3.1.3, a barred structure may induce a cylindrical rotation of the bulge (Saha et al. 2011).

Recently, some observations showed bimodal metallicity distributions and kinematics among MW bulge stars, implying a multiple formation process of the MW bulge (Babusiaux et al. 2010; Bensby et al. 2010b, 2011b; Hill et al. 2011). Babusiaux et al. (2010) and Hill et al. (2011) suggested that the MW bulge is a complex bulge of a classical bulge and a pseudobulge. Thus, bulge formation in real galaxies (including the MW) might be complex and proceed through multiple scenarios. Some bulges would be a composite structure as proposed by some observations of extra-galaxies (e.g. Erwin et al. 2003; Kormendy et al. 2010; Kormendy & Barentine 2010; Fisher & Drory 2011).

Such unclassifiable bulges like the MW bulge (old pseudobulge) are also observed in some other disc galaxies (e.g. Bica & Alloin 1987; Peletier et al. 1999). Our simulation results suggest that clump-origin bulges could be a possible origin of these old pseudobulges. In addition, as we discussed in §3.4, the inactive pseudobulges may be also clump-origin bulges.

4.3 Exponential bulges in the high-redshift Universe

It is very difficult to determine whether a bulge observed in a distant disc galaxy is clump-origin or not. Although Kormendy & Kennicutt (2004) has argued that the secular evolution could build some pseudobulges quickly $\gtrsim 5$ Gyr ago, we expect that the secular evolution would not be able to build up a pseudobulge in a premature disc in early phase of the galaxy formation. It is because the ‘*secular*’ evolution has to postdate accomplishment of their disc formation and takes a long time to form a pseudobulge. Therefore, we can expect that a galactic bulge observed in the high-redshift Universe would be either a classical bulge or a clump-origin bulge. As we showed in §3.1.1, the clump-origin bulge has a nearly exponential surface density profile, which is distinguishable from the $R^{1/4}$ law profile of the classical bulges. Thus, if the density profile of the bulges in clump clusters could be observationally resolved, we would be able to identify the clump-origin bulges by identifying their exponential density profile.

Elmegreen et al. (2007) has observationally indicated that comoving spatial number density of clumpy galaxies (clump clusters and chain galaxies) in the high-redshift Universe ($1 \lesssim z \lesssim 4$) are consistent with the density of spiral galaxies in the nearby Universe and suggested that quite a few galaxies of current spirals used to be a clump cluster or a chain galaxy. This implies that disc galaxies hosting a clump-origin bulge may not be rare. However, the idea that all disc galaxies must have formed a clump-origin bulge contradicts the observational fact that the number of bulge-less spiral galaxies is not small (Kormendy et al. 2010; Fisher & Drory 2011). As we noted in §4.1, Elmegreen & Elmegreen (2005) had discussed that the observed clump clusters could not be the nearby spiral galaxies because of the too high surface density.

4.4 Comparison with previous studies

So far, there have been only a few studies discussing the natures of clump-origin bulges. As we noted in §3.1, Elmegreen et al. (2008) has argued with numerical simulations that clump-origin bulges have a similar dynamical state to classical bulges, such as a large Sérsic index, $n \gtrsim 2$ and a slow rotation, $V/\sigma_0 \simeq 0.4 - 0.5$. Their results indicating classical bulge-like signatures poses a discrepancy with our results. This disagreement may imply that the properties of clump-origin bulges depend on initial conditions of simulations. Our simulation model adopted the collapsing gas sphere model, while Elmegreen et al. (2008) used a uniform density disc model as their initial condition. As we discussed, the size and number of the clumps would depend on the initial spin parameter. The size of the clumps may affect the relaxation process in the clump mergers. In the simulations of Elmegreen et al. (2008), fewer and larger clumps form in the clump cluster and the resultant B/T ratio is somewhat larger than in our simulation.

Simulation method may also be a possible cause of the disagreement. The simulations of Elmegreen et al. (2008) were performed by a particle-mesh sticky-particle code which mimics hydrodynamics by inelastic collisions between particles designated as a gas particle. On the other

hand, we describe the multi-phase interstellar medium with our SPH code which treats radiative cooling, far-ultraviolet heating and SN feedback with hydrodynamical equations of motion. Since the sticky particle method is only an imitation of hydrodynamics, the evolution of the ISM represented by the sticky-particle method may lead different from that by the SPH method. The SPH simulations have also still suffered from the overcooling problem (e.g. Katz & Gunn 1991; Navarro & Benz 1991; Navarro & White 1994; Thoul & Weinberg 1995, 1996; Okamoto et al. 2005; Sawala et al. 2011). Degree of dissipation, i.e. richness of gas, in merging clumps may also affect the properties of the clump-origin bulge. Moreover, structure of remnants seems to depend on the equation of state and cooling of gas (Bournaud et al. 2011). Hence, the contradiction of our results of the clump-origin bulge to that of Elmegreen et al. (2008) may stem from a difference of gaseous physics in the clump merger. The degree of dissipation in the clump mergers may depend on initial conditions of a simulation model and/or the adopted numerical scheme for hydrodynamics (the sticky-particle or SPH code).

As noted above, the clump-origin bulge in our simulation has nearly twice larger rotation in terms of V_{\max}/σ_0 than the result of Elmegreen et al. (2008). Recently, the simulations of Aumer et al. (2010) and Ceverino et al. (2011) have also demonstrated that the clumps in clump clusters are dynamically rotation supported systems during the migration toward the galactic centre although they paid little attention to resultant bulges. Especially, Ceverino et al. (2011) mentioned that clumps which have experienced merger with other clumps tend to be highly supported by rotation and indicated that more massive clumps have larger rotation (their §4.2). Although Ceverino et al. (2011) discussed kinematics of gas only, their results imply that the clump merger can spin up the remnant clumps. Therefore, we could expect that the clump-origin bulges in their simulations would have a significant rotation because the clump-origin bulges are the final remnant of the clump mergers.

Clump-origin bulges form through ‘*mergers of stellar clumps*’ in a disc, whereas classical bulges form through ‘*mergers of galaxies*’. Formation of the clumps are caused by instability of gas in rotating disc, therefore, these clumps retain a memory of their discy origin and a spin in the same direction as the disc rotation as shown by Ceverino et al. (2011). The bulge formation by the clump mergers takes place in the disc plane after orbiting around the galactic centre in the same direction, i.e. ‘*prograde-prograde merger*’. As a result, the clump-origin bulges which are remnant of the clump merger retain the orbital angular momentum of the merger and the spin angular momentum of the progenitor clumps in their kinematics. Then, the bulges should acquire the significant rotation of which property is different from that of classical bulges although both of them are built through merger-origin formation scenarios.

Our result indicated the nearly exponential surface density profile with the Sérsic index of $n = 1.18$. We speculate that this exponential profile may stem from the elongated bar-like shape of the bulge in our simulation (Fig. 4). It has been observed that barred structures in spiral galaxies have an exponential density profile (e.g. Elmegreen & Elmegreen 1985; Ohta et al. 1990). This was demonstrated also using

numerical simulations by Combes & Elmegreen (1993) and Noguchi (1996)⁵.

5 SUMMARY

We summarize the natures of the clump-origin bulge in our simulation:

- nearly exponential surface density profile,
- elongated bar-like structure, and boxy shape,
- significant net rotation, but not cylindrical,
- old stellar population,
- high metallicity of stars with vertical gradient and
- inactive star formation (if there is no late accretion).

If we compare these natures with those observed in typical classical bulge and pseudobulges (Kormendy & Kennicutt 2004), the former three natures, exponential profile, boxy shape and a significant rotation, indicate pseudobulge-like signatures. On the other hand, the latter three, old, metal-rich stars and weak star formation, represent classical bulge-like signatures. Therefore, the clump-origin bulge, which we obtained here, can not be simply classified into classical bulges nor pseudobulges, but should have unique properties as shown in this paper.

However, Elmegreen et al. (2008) has suggested with numerical simulations that clump-origin bulges should be a classical bulge. This inconsistency would be due to adopting different initial conditions and/or numerical schemes. As we discussed in §3.1.1 and 4, initial setup in simulations would control disc diameters, gas density in the disc and the size of clump-origin bulges finally, and may affect the natures of the clump-origin bulge.

Hence, our results open up a different possibility of clump-origin bulges than the result of Elmegreen et al. (2008). In our simulation, the surface density of the disc is lower and the resultant bulge is smaller than Elmegreen et al. (2008). Therefore, it is expected that low surface brightness clump clusters prefer a *clump-origin pseudobulge* and enable the galaxy to avoid the *clump-origin classical bulge* formation. The clump-origin pseudobulge is more applicable to the MW bulge which is a pseudobulge-like but old metal-rich bulge. The low surface brightness clump clusters might had been present but missed in the observations and Elmegreen & Elmegreen (2005) discussed that clump clusters in their observation have a too high surface density to be the MW progenitor. Thus, to investigate the clump-origin bulge formation and its natures may take an important role to seek the formation history of the MW.

ACKNOWLEDGMENTS

We thank Frédéric Bournaud for his fascinating suggestions as the reviewer, who kindly helped improve the paper. We are grateful to Daisuke Kawata for polishing up the paper,

⁵ He proposed that spontaneous bars have an exponential profile, tidal bars have a flat one, in agreement with observations.

Masafumi Noguchi for his helpful discussion. S.I. is financially supported by Research Fellowships of the Japan Society for the Promotion of Science (JSPS) for Young Scientists. The numerical simulations reported here were carried out on Cray XT-4 kindly made available by CfCA (Center for Computational Astrophysics) at the National Astronomical Observatory of Japan. This project is partly supported by HPCI Strategic Program Field 5 ‘The origin of matter and the universe’.

REFERENCES

- Abadi M. G., Navarro J. F., Steinmetz M., Eke V. R., 2003, *ApJ*, 597, 21
- Agertz O., Teyssier R., Moore B., 2009, *MNRAS*, 397, L64
- Allende Prieto C., Beers T. C., Wilhelm R., Newberg H. J., Rockosi C. M., Yanny B., Lee Y. S., 2006, *ApJ*, 636, 804
- Alves-Brito A., Meléndez J., Asplund M., Ramírez I., Yong D., 2010, *A&A*, 513, A35+
- Athanassoula E., 2005, *MNRAS*, 358, 1477
- Aumer M., Burkert A., Johansson P. H., Genzel R., 2010, *ApJ*, 719, 1230
- Babusiaux C., et al., 2010, *A&A*, 519, A77+
- Baron E., White S. D. M., 1987, *ApJ*, 322, 585
- Bate M. R., Burkert A., 1997, *MNRAS*, 288, 1060
- Bekki K., Freeman K. C., 2002, *ApJL*, 574, L21
- Bensby T., Alves-Brito A., Oey M. S., Yong D., Meléndez J., 2010a, *A&A*, 516, L13+
- Bensby T., Alves-Brito A., Oey M. S., Yong D., Meléndez J., 2011a, *ApJL*, 735, L46+
- Bensby T., et al., 2009, *A&A*, 499, 737
- Bensby T., et al., 2010b, *A&A*, 512, A41+
- Bensby T., et al., 2011b, *A&A*, 533, A134+
- Bica E., Alloin D., 1987, *A&AS*, 70, 281
- Binny J., Tremaine S., 2008, *Galactic Dynamics Second Edition*. Princeton Univ. Press, Princeton
- Bouché N., et al., 2007, *ApJ*, 671, 303
- Bournaud F., Elmegreen B. G., Elmegreen D. M., 2007, *ApJ*, 670, 237
- Bournaud F., Elmegreen B. G., Martig M., 2009, *ApJL*, 707, L1
- Bournaud F., et al., 2011, *ApJ*, 730, 4
- Brook C. B., Gibson B. K., Martel H., Kawata D., 2005, *ApJ*, 630, 298
- Brook C. B., Kawata D., Gibson B. K., Freeman K. C., 2004, *ApJ*, 612, 894
- Bullock J. S., Dekel A., Kolatt T. S., Kravtsov A. V., Klypin A. A., Porciani C., Primack J. R., 2001, *ApJ*, 555, 240
- Burkert A., Truran J. W., Hensler G., 1992, *ApJ*, 391, 651
- Burstein D., Bender R., Faber S., Nolthenius R., 1997, *AJ*, 114, 1365
- Cappellari M., et al., 2007, *MNRAS*, 379, 418
- Ceverino D., Dekel A., Bournaud F., 2010, *MNRAS*, 404, 2151
- Ceverino D., Dekel A., Mandelker N., Bournaud F., Burkert A., Genzel R., Primack J., 2011, preprint (astro-ph/1106.5587)
- Combes F., Elmegreen B. G., 1993, *A&A*, 271, 391
- Combes F., Sanders R. H., 1981, *A&A*, 96, 164
- de Vaucouleurs G., 1948, *Annales d’Astrophysique*, 11, 247
- Debattista V. P., Carollo C. M., Mayer L., Moore B., 2004, *ApJL*, 604, L93
- Drory N., Fisher D. B., 2007, *ApJ*, 664, 640
- Dutton A. A., et al., 2011, *MNRAS*, 410, 1660
- Dwek E., et al., 1995, *ApJ*, 445, 716
- Elmegreen B. G., Bournaud F., Elmegreen D. M., 2008, *ApJ*, 688, 67
- Elmegreen B. G., Elmegreen D. M., 1985, *ApJ*, 288, 438
- Elmegreen B. G., Elmegreen D. M., 2005, *ApJ*, 627, 632
- Elmegreen D. M., Elmegreen B. G., Hirst A. C., 2004, *ApJL*, 604, L21
- Elmegreen D. M., Elmegreen B. G., Marcus M. T., Shahinyan K., Yau A., Petersen M., 2009, *ApJ*, 701, 306
- Elmegreen D. M., Elmegreen B. G., Ravindranath S., Coe D. A., 2007, *ApJ*, 658, 763
- Erwin P., Beltrán J. C. V., Graham A. W., Beckman J. E., 2003, *ApJ*, 597, 929
- Fall S. M., Efstathiou G., 1980, *MNRAS*, 193, 189
- Ferreras I., Wyse R. F. G., Silk J., 2003, *MNRAS*, 345, 1381
- Fisher D. B., 2006, *ApJL*, 642, L17
- Fisher D. B., Drory N., 2008, *AJ*, 136, 773
- Fisher D. B., Drory N., 2010, *ApJ*, 716, 942
- Fisher D. B., Drory N., 2011, *ApJL*, 733, L47+
- Fisher D. B., Drory N., Fabricius M. H., 2009, *ApJ*, 697, 630
- Frogel J. A., Terndrup D. M., Blanco V. M., Whitford A. E., 1990, *ApJ*, 353, 494
- Fulbright J. P., McWilliam A., Rich R. M., 2007, *ApJ*, 661, 1152
- Genel S., et al., 2010, preprint (astro-ph/1011.0433)
- Genzel R., et al., 2011, *ApJ*, 733, 101
- Gonzalez O. A., et al., 2011a, *A&A*, 530, A54+
- Gonzalez O. A., Rejkuba M., Zoccali M., Valenti E., Minniti D., 2011b, *A&A*, 534, A3+
- Hill V., et al., 2011, *A&A*, 534, A80+
- Hopkins P. F., et al., 2010, *ApJ*, 715, 202
- Howard C. D., et al., 2009, *ApJL*, 702, L153
- Hubber D. A., Goodwin S. P., Whitworth A. P., 2006, *A&A*, 450, 881
- Immeli A., Samland M., Gerhard O., Westera P., 2004a, *A&A*, 413, 547
- Immeli A., Samland M., Westera P., Gerhard O., 2004b, *ApJ*, 611, 20
- Inoue S., Saitoh T. R., 2011, preprint (astro-ph/1108.0906)
- Ivezić Ž., et al., 2008, *ApJ*, 684, 287
- Jablonka P., Martin P., Arimoto N., 1996, *AJ*, 112, 1415
- Johnson C. I., Rich R. M., Fulbright J. P., Valenti E., McWilliam A., 2011, *ApJ*, 732, 108
- Katz N., Gunn J. E., 1991, *ApJ*, 377, 365
- Kaufmann T., Mayer L., Wadsley J., Stadel J., Moore B., 2006, *MNRAS*, 370, 1612
- Kaufmann T., Mayer L., Wadsley J., Stadel J., Moore B., 2007, *MNRAS*, 375, 53
- Kent S. M., 1992, *ApJ*, 387, 181
- Kent S. M., Dame T. M., Fazio G., 1991, *ApJ*, 378, 131
- Kimm T., Devriendt J., Slyz A., Pichon C., Kassin S. A., Dubois Y., 2011, preprint (astro-ph/1106.0538)
- Kormendy J., 1985, *ApJ*, 295, 73
- Kormendy J., Barentine J. C., 2010, *ApJL*, 715, L176
- Kormendy J., Drory N., Bender R., Cornell M. E., 2010, *ApJ*, 723, 54

- Kormendy J., Illingworth G., 1982, *ApJ*, 256, 460
 Kormendy J., Illingworth G., 1983, *ApJ*, 265, 632
 Kormendy J., Kennicutt Jr. R. C., 2004, *ARA&A*, 42, 603
 Krumholz M. R., Dekel A., 2010, *MNRAS*, 406, 112
 Lecureur A., Hill V., Zoccali M., Barbuy B., Gómez A., Minniti D., Ortolani S., Renzini A., 2007, *A&A*, 465, 799
 Makino J., 2004, *PASJ*, 56, 521
 McWilliam A., Rich R. M., 1994, *ApJS*, 91, 749
 McWilliam A., Zoccali M., 2010, *ApJ*, 724, 1491
 Meléndez J., et al., 2008, *A&A*, 484, L21
 Monaghan J. J., 1992, *ARA&A*, 30, 543
 Naab T., Trujillo I., 2006, *MNRAS*, 369, 625
 Nagashima M., Okamoto T., 2006, *ApJ*, 643, 863
 Nakasato N., Nomoto K., 2003, *ApJ*, 588, 842
 Nataf D. M., Udalski A., 2011, preprint (astro-ph/1106.0005)
 Nataf D. M., Udalski A., Gould A., Fouqué P., Stanek K. Z., 2010, *ApJL*, 721, L28
 Navarro J. F., Benz W., 1991, *ApJ*, 380, 320
 Navarro J. F., Frenk C. S., White S. D. M., 1997, *ApJ*, 490, 493
 Navarro J. F., White S. D. M., 1994, *MNRAS*, 267, 401
 Noguchi M., 1996, *ApJ*, 469, 605
 Noguchi M., 1998, *Nat*, 392, 253
 Noguchi M., 1999, *ApJ*, 514, 77
 Ohta K., Hamabe M., Wakamatsu K.-I., 1990, *ApJ*, 357, 71
 Okamoto T., Eke V. R., Frenk C. S., Jenkins A., 2005, *MNRAS*, 363, 1299
 Okamoto T., Nemmen R. S., Bower R. G., 2008, *MNRAS*, 385, 161
 Peletier R. F., Balcells M., Davies R. L., Andredakis Y., Vazdekis A., Burkert A., Prada F., 1999, *MNRAS*, 310, 703
 Pfenninger D., Norman C., 1990, *ApJ*, 363, 391
 Quinn P. J., Hernquist L., Fullagar D. P., 1993, *ApJ*, 403, 74
 Rahimi A., Kawata D., Brook C. B., Gibson B. K., 2010, *MNRAS*, 401, 1826
 Rich R. M., Origlia L., Valenti E., 2007, *ApJL*, 665, L119
 Ruchti G. R., et al., 2011, *ApJ*, 737, 9
 Ryde N., et al., 2010, *A&A*, 509, A20+
 Saha K., Martinez-Valpuesta I., Gerhard O., 2011, preprint (astro-ph/1105.5797)
 Sahu K. C., et al., 2006, *Nat*, 443, 534
 Saito R. K., Zoccali M., McWilliam A., Minniti D., Gonzalez O. A., Hill V., 2011, *AJ*, 142, 76
 Saitoh T. R., Daisaka H., Kokubo E., Makino J., Okamoto T., Tomisaka K., Wada K., Yoshida N., 2008, *PASJ*, 60, 667
 Saitoh T. R., Daisaka H., Kokubo E., Makino J., Okamoto T., Tomisaka K., Wada K., Yoshida N., 2009, *PASJ*, 61, 481
 Saitoh T. R., Makino J., 2009, *ApJL*, 697, L99
 Saitoh T. R., Makino J., 2010, *PASJ*, 62, 301
 Salpeter E. E., 1955, *ApJ*, 121, 161
 Sawala T., Guo Q., Scannapieco C., Jenkins A., White S., 2011, *MNRAS*, 413, 659
 Schmidt M., 1959, *ApJ*, 129, 243
 Sellwood J. A., Binney J. J., 2002, *MNRAS*, 336, 785
 Springel V., 2010, *ARA&A*, 48, 391
 Terndrup D. M., 1988, *AJ*, 96, 884
 Terndrup D. M., Frogel J. A., Whitford A. E., 1990, *ApJ*, 357, 453
 Thoul A. A., Weinberg D. H., 1995, *ApJ*, 442, 480
 Thoul A. A., Weinberg D. H., 1996, *ApJ*, 465, 608
 Toomre A., 1964, *ApJ*, 139, 1217
 van den Bergh S., Abraham R. G., Ellis R. S., Tanvir N. R., Santiago B. X., Glazebrook K. G., 1996, *AJ*, 112, 359
 van den Bergh S., Herbst E., 1974, *AJ*, 79, 603
 Wada K., Papadopoulos P. P., Spaans M., 2009, *ApJ*, 702, 63
 Williams M. J., Zamojski M. A., Bureau M., Kuntschner H., Merrifield M. R., de Zeeuw P. T., Kuijken K., 2011, *MNRAS*, 414, 2163
 Wyse R. F. G., Gilmore G., Franx M., 1997, *ARA&A*, 35, 637
 Zoccali M., et al., 2006, *A&A*, 457, L1
 Zoccali M., Hill V., Lecureur A., Barbuy B., Renzini A., Minniti D., Gómez A., Ortolani S., 2008, *A&A*, 486, 177